improvements in throughput efficiency by means of II-GHARQ are almost the same for both KM and DC codes.

Common decoding—Hadamard transform decoding:[4] Generally speaking, the decoders for all (ni, n, d_i) codes are different. The decoders in II-GHARQ receivers will be simplified if decoding of each (ni, n) code can be completed by the same decoder. The KM codes do have this property which is, however, a reason why KM codes possess poor DDSs. We recommend that Hadamard transform decoding can be regarded as a common decoding for all codes whose n is small, for example the codes listed in Table 2. Hadamard transform decoding is a maximum-likelihood decoding scheme and is well suited for soft-decision decoding.

Simulation results: In the simulation we assume that the scheme is selectively retransmittive and buffer sizes in the transmitter and receiver are infinite. The channel uses 2-PSK modulation with independent additive Gaussian noise. Decoders may use hard-decision output or analogue output of the demodulator. $N = 250$ and $n = 5$, (10, 5) DC code, (15, 5) MDC code and (15, 5) KM code are adopted. The simulation results are shown in Fig. 1, in which the vertical axis represents throughput efficiency T and the horizontal axis represents the bit error rate of the schemes, P_b.

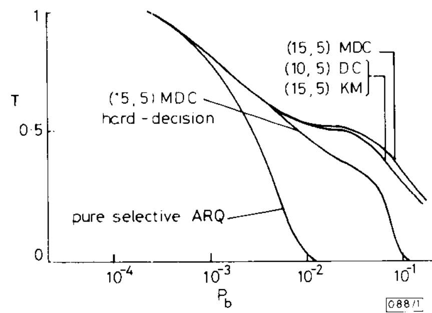

Fig. 1 *Throughput of various codes*

Fig. 1 indicates the following:

(1) The throughputs of II-HARQ and II-GHARQ are better than pure selective ARQ when the bit error rate becomes larger than 10^{-2}.

(2) Analogue or soft-decision decoding can improve the throughput further when the channel becomes much worse or, in other words, have better robustness.

(3) Differences in the throughput between the (10, 5) DC code, (15, 5) MDC code and (15, 5) KM code are fairly small, although the (15, 5) MDC code gives the best throughput efficiency. This illustrates that II-GHARQ has almost no further improvement on the throughput compared to II-HARQ using the DC codes, which may be the best choice from the viewpoint of trade-off between performance and complexity.

MA JIANHUA
WANG XINMEI

Department of Information Engineering
Xidian University
Xi'an, People's Republic of China

17th October 1989

References

1 METZNER, J. J., and CHANG, D.: 'Efficient selective repeat ARQ strategies for very noisy and fluctuating channels', *IEEE Trans.*, 1985, **COM-33**, pp. 409–415
2 KRISHNA, H., and MORGERA, S. D.: 'A new error control scheme for hybrid ARQ systems', *ibid.*, 1987, **COM-35**, pp. 981–990
3 MORGERA, S. D., and ODUOL, V. K.: 'Soft-decision decoding applied to the generalized type-II hybrid ARQ scheme', *ibid.*, 1989, **COM-37**, pp. 393–396
4 BEERY, Y., and SNYDERS, J.: 'Optimal soft decision block decoders based on fast Hadamard transform', *ibid.*, 1986, **IT-32**, pp. 355–364

EXTREMELY LOW-RESISTANCE NONALLOYED OHMIC CONTACTS ON MOLECULAR BEAM EPITAXIALLY GROWN *p*-TYPE Ge

Indexing terms: Semiconductor devices and materials, Semiconductor growth, Semiconductors, GaAs

Extremely low-resistance nonalloyed ohmic contacts have been formed on *p*-type Ge grown on GaAs by molecular beam epitaxy as part of a research effort into GaAs/Ge heterojunction devices. Using evaporated Ti/Al metallisation, specific contact resistances well below $1 \times 10^{-8}\,\Omega\,cm^2$ were achieved for heavily doped Ge ($p > 1 \times 10^{19}\,cm^{-3}$). The investigated Ge layers were grown as the base region of AlGaAs/Ge/GaAs HBTs. The influence of the low base resistance on the high-frequency performance of HBTs was studied by simulations.

A variety of material systems, device structures and fabrication techniques have been investigated to improve the performance of heterojunction bipolar transistors (HBTs) over the years. Some critical parameters affecting the device performance are base doping, base contact resistance and band discontinuity at the base/emitter interface. The use of Ge as a base material has great potential to improve the performance of GaAs/AlGaAs HBTs due to its large doping-mobility product and favourable band discontinuities with GaAs. Heavily doped Ge can be used as a low-resistance base for HBTs in the GaAS material system.[1,2] Earlier we reported excellent diode characteristics for *p*-Ge/*n*-(GaAs, AlGaAs) junctions,[3] and demonstrated a high-gain AlGaAs/Ge/GaAs HBT.[1] In this letter we would like to discuss the contact resistances on *p*-Ge and its influence on the high-frequency performance of HBTs.

The GaAs growth was done in a Perkin Elmer 430 molecular beam epitaxy (MBE) system while Ge deposition took place in an adjacent chamber to minimise cross-contamination. Samples remained under vacuum during the several minutes of growth interruption required to transfer samples between chambers. All sources were solid source effusion cells. An initial buffer layer of 1 µm Si-doped GaAs was grown with a carrier concentration of $N = 4 \times 10^{18}\,cm^{-3}$ on a semi-insulating GaAs (100) substrate. Next, 0·4 µm of GaAs was deposited with a lighter Si doping of $N = 5 \times 10^{16}\,cm^{-3}$. Finally, 500–700 Å of Ge was grown, the growth being interrupted several times for Ga delta doping to hole concentrations of 4×10^{18} to $4 \times 10^{19}\,cm^{-3}$. These structures were grown to simulate the base–collector junctions of HBTs. Some of the samples were annealed at 700°C prior to fabrication to enhance donor activation in the Ge. Standard photolithographic techniques were used to form contact patterns on Ge.

Chemical palladium (Pd) plating was employed to facilitate ohmic contacts on *p*-Ge in the preliminary part of this study, resulting in specific contact resistance values as low as mid-$10^{-8}\,\Omega\,cm^2$. However, due to drawbacks related to this process, such as metal and contact resistance nonuniformity, uncontrolled thickness of metallisation, high eelctrical resistivity of Pd (10·54 µΩ cm compared to 2·65 µΩ cm for Al), and the impossibility of forming self-aligned contacts, we elected to evaporate Ti/Al with a subsequent liftoff for ohmic contact formation. As a compromise between the metal sheet resistance (much smaller for Al than Ti) and liftoff difficulties associated with very thick metallisation, a 300 Å Ti/3500 Å Al metallisation was chosen.

Contact resistances were measured using the well established transmission line model (TLM) method.[4] The test pattern consists of rectangular pads, 80 µm long and 250 µm wide, separated by a gap varying from 1 to 20 µm. The exact contact spacing and width were carefully calibrated by optical microscopy for each TLM pattern, since the main error in measurements arises from the length determination. A potentially greater error, introduced by the TLM model, may arise from the assumption that the thickness of the conducting channel approaches zero. However, for the investigated structures (very thin and highly conducting Ge), we estimate the experimental uncertainty introduced by this assumption of the

extended TLM model[5] to range from low to mid-$10^{-9}\,\Omega\,cm^2$ for the doping levels used. A four-point probe arrangement was employed to eliminate any possible error introduced by the probe contact resistance. A constant current of 1 mA was applied in all measurements, and the resistance was demonstrated to be independent of the applied current.

The specific contact resistivity and sheet resistivity were derived from a plot of the measured resistance against gap spacing, as shown in Fig. 1. The method of least squares was used to obtain a straight line fit to the experimental data. From the y-axis intercept of the line and the slope, the contact resistance and the sheet resistance were calculated, respectively.

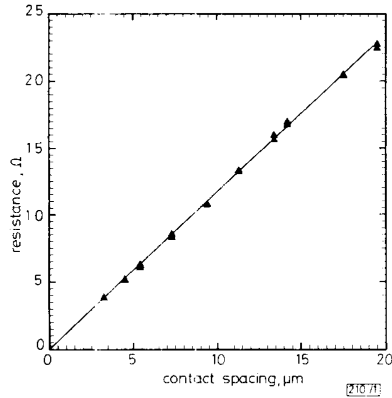

Fig. 1 *Plot of transmission line method data of nonalloyed Ti/Al ohmic contacts for sample 3*

Table 1 summarises the measured sheet and contact resistivities for the samples along with the estimated dopant concentrations. Specific contact resistance values less than $1 \times 10^{-8}\,\Omega\,cm^2$ should be viewed carefully as the error margin for measurements is approached. However, the decreasing trend of contact resistance with decreasing sheet resistance suggests specific contact resistance values well below $1 \times 10^{-8}\,\Omega\,cm^2$.

Postmetallisation heat treatment was used to test thermal stability of the Ti/Al contacts. Up to 400°C no change in the contact resistances and minimal change in surface morphology were observed. After sintering at 400°C for 5 min the contact resistances increased drastically and became nonuniform. Current/voltage characteristics of the p-Ge/N-GaAs junction were measured before and after sintering and no change was observed, thus eliminating the possibility of Ti diffusion into Ge. These high contact resistances are likely to be due to the formation of $TiAl_3$ at the Al/Ti interface. For similar contacts on Si, this reaction was observed when the temperature exceeded 350°C,[6] which is consistent with our findings. If the entire Ti layer is consumed in this reaction the desirable contact is then lost.[6] The thermal stability of these contacts can be improved by means of increasing the Ti thickness.

To emphasise the importance of low contact resistances, we would like to compare the resistance values obtained on p-Ge to that on p-GaAs. Typical specific resistance values obtained in our laboratory for p-type contacts on GaAs are in the order of $10^{-6}\,\Omega\,cm^2$. Employing a GaSb/GaAs strained-layer superlattice and a GaSb cap, specific contact resistivities as low as $3 \cdot 2 \times 10^{-7}\,\Omega\,cm^2$ have been reported[7] for nonalloyed contacts. However, this technique requires regrowth if applied to p-type bases for HBTs, and a very clean sample surface was necessary prior to metallisation.[7] For Ti/Al contacts on Ge no cleaning procedures were used before evaporation, and uniform low resistance contacts were realised.

Fig. 2 shows the results of simulations which investigated the dependence of maximum oscillation frequency f_{max} and minimum noise figure F_{min} at 30 GHz on the specific base contact resistance for an AlGaAs/Ge/GaAs HBT. It is clear that the low contact resistances attainable through the use of a Ge base offer significant improvement over a conventional GaAs base. Note that at the low resistance end of the plot, f_{max} and F_{min} start to saturate, and further reduction of the contact resistance will not improve the performance drastically. Thus, there is no need for further improvement over these contact resistances for practical device applications.

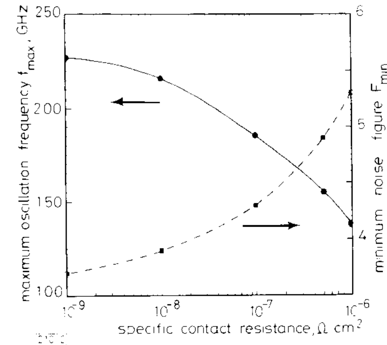

Fig. 2 *Dependence of f_{max} and F_{min} (at 30 GHz) on base contact resistance for AlGaAs/Ge/GaAs HBT with base doping of $1 \times 10^{19}\,cm^{-3}$, base thickness of 750 Å and emitter stripe width of 1 μm*

Bias conditions are chosen as collector current density = $5 \times 10^4\,A/cm^2$, collector base potential = 2 V

In conclusion, we have demonstrated thermally stable, extremely low-resistance nonalloyed Ti/Al ohmic contacts on p-Ge. With the continuing reduction of device geometries, the use of nonalloyed ohmic contacts becomes crucial to avoid the lateral and vertical diffusion associated with high-temperature processing. Very low nonalloyed contact resistance and its implications on the high-frequency performance of HBTs indicate that the p-Ge base is an excellent candidate to replace GaAs in HBTs.

This research is supported by the Air Force Office of Scientific Research (grant AFOSR-89-0239), the SDIO IST Office through ONR (grant N00014-86-K-0513) and the National Science Foundation under contract ECS-88-22406. One of us (SS) wishes to acknowledge the support of an NSF graduate fellowship.

M. S. ÜNLÜ
S. STRITE
K. ADOMI
G. B. GAO
H. MORKOÇ

Material Science Laboratory
& Coordinated Science Laboratory
University of Illinois at Urbana-Champaign
1101 W. Springfield Avenue, Urbana, IL 61801, USA

7th November 1989

References

1 STRITE, S., ÜNLÜ, M. S., ADOMI, K., GAO, G. B., and MORKOÇ, H.: 'AlGaAs/Ge/GaAs heterojunction bipolar transistors grown by molecular beam epitaxy', *IEEE Electron Dev. Lett.*, in press

Table 1 MEASURED SHEET AND SPECIFIC TRANSFER RESISTANCES, AND CALCULATED SPECIFIC CONTACT RESISTANCES FOR DIFFERENT LAYERS WITH ESTIMATED DOPING DENSITIES

Layer	1	2	3	4
Ge doping N_A, cm^{-3}	4×10^{18}	7×10^{18}	2×10^{19}	4×10^{19}
Sheet resistance, Ω/□	800	650	290	215
Specific trans. R, Ω mm	0·03	0·024	<0·01	<0·01
Specific contact R, Ω cm²	$1 \cdot 2 \times 10^{-8}$	9×10^{-9}	$<5 \times 10^{-9}$	$<5 \times 10^{-9}$

2 KIMURA, T., KAWANAKA, M., and SONE, J.: 'MBE-grown Ge/GaAs heterojunction bipolar transistors operated at 300 K and 77 K with current gain of 45'. 47th IEEE dev. res. conf., 19th–21st June 1989, Cambridge, MA, Paper IIA-8
3 ÜNLÜ, M. S., STRITE, S., GAO, G. B., ADOMI, K., and MORKOÇ, H.: 'Electrical characteristics of p^+-Ge/(N-GaAs and N-AlGaAs) junctions and their applications to Ge base transistors', submitted to *Appl. Phys. Lett.*
4 BERGER, H. H.: 'A transmission line model for contacts to planar devices'. Tech. dig. of IEEE int. solid-state circuits conf., 19th–21st Feb. 1969, Philadelphia, PA (IEEE, NY), pp. 160–162
5 BERGER, H. H. 'Models for contacts to planar devices', *Solid-State Electron.*, 1972, **15**, pp. 145–158
6 BOWER, W. R.: 'Characteristics of aluminum-titanium electrical contacts on silicon', *Appl. Phys. Lett.*, 1973, **23**, pp. 99–101
7 CHYI, J.-L., CHEN, J., KUMAR, N. S., KIELY, C., PENG, C. K., ROCKETT, A., and MORKOÇ, H.: 'Low resistance nonalloyed ohmic contacts on p-type GaAs using GaSb/GaAs strained layer superlattices', *ibid.*, 1989, **55**, pp. 570–571

94 GHz InP MMIC FIVE-SECTION DISTRIBUTED AMPLIFIER

Indexing terms: Semiconductor devices and materials, Integrated circuits, Amplifiers, Microwave amplifiers

A single-stage 94 GHz InP MMIC amplifier with 6·4 dB gain at 94 GHz has been developed, which is the highest-frequency MMIC amplifier reported to date. Lattice-matched GaInAs/AlInAs HEMTs with 0·1 μm mushroom gates were the active devices. The CPW MMIC chip dimensions are 500 μm × 670 μm.

Introduction: Monolithic millimetre-wave integrated circuits (MMICs) will be the key to high-volume and very small, commercial and military millimetre-wave systems. Because of low atmospheric absorption at 94 GHz, systems operating at this frequency are of particular interest for communications and radar applications. Recently, InP-based HEMTs were used in a hybrid configuration to demonstrate amplification at 94 GHz.[1] MMIC amplifiers, however, have only been demonstrated to 65 GHz with GaAs-based HEMTs.[2] The only InP MMIC amplifier, which was reported recently, has a 26–40 GHz bandwidth.[3] We report an InP-based 94 GHz MMIC amplifier implemented in coplanar waveguide (CPW), with 6·4 dB gain at 94 GHz. Although 100 GHz CPW frequency-multipliers and harmonic mixers have been previously demonstrated,[4,5] this work also shows the application of CPWs in MMIC amplifiers at W-band (75–110 GHz).

Device characteristics: The material structure of the active device is shown in Fig. 1*a*. The active channel was undoped GaInAs, lattice-matched to InP with AlInAs, also lattice-matched to InP as the barrier material. The 0·1 μm gate length had a mushroom structure, and was defined by e-beam lithography. Fig. 1*b* shows a scanning electron microscope (SEM) photograph of the 0·1 μm mushroom gate. The maximum frequency of oscillation F_{max} of this device was in excess of 200 GHz, based on its equivalent circuit model derived from 1–40 GHz measured *S*-parameters. The extrapolated F_t for the devices in this MMIC was in excess of 90 GHz.

Circuit design: The schematic circuit diagram of the five-section distributed amplifier is shown in Fig. 2*a*. There are five 0·1 μm HEMTs with a total gate periphery of 122 μm. CPW is used to form the artificial gate and drain transmission lines, and for phase equalisation of the signal on the drain transmission line. A microphotograph of the MMIC chip is shown in Fig. 2*b*. The overall MMIC chip dimensions are 500 μm × 670 μm.

MMIC fabrication: The MMIC had five HEMTs, two thin-film resistors and two parallel-plate MIM capacitors. TaN

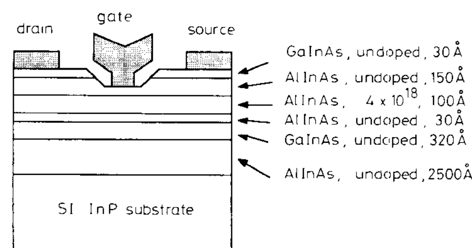

a

[3147/1]

b [3147/1]

Fig. 1

a Material structure of W-band InP HEMT
b SEM photograph of 0·1 μm gate of W-band InP HEMT

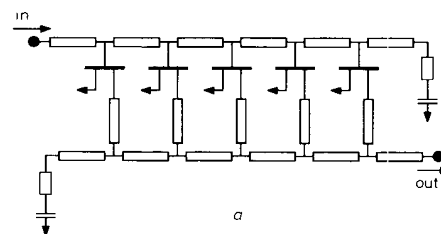

a

[3147/2]

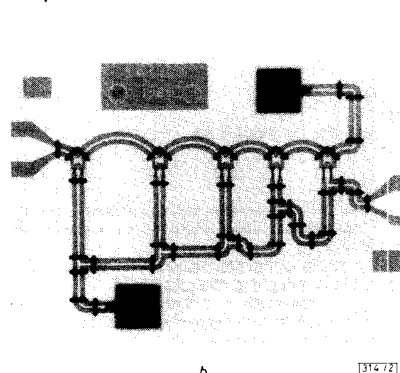

b [3147/2]

Fig. 2

a Schematic circuit diagram of 94 GHz MMIC five-section distributed amplifier
b Photograph of 94 GHz MMIC five-section distributed amplifier